Supplementary Information

Effect of impurities in different activated carbon materials and their in-depth electrochemical analysis of supercapacitor coin-cell device in organic electrolyte†

Kye-yeol Lee [a], Il Yeong Jeong [a], Jeong-Woo Kim [a], Seungmin Yu [b], Hye-Min Lee [c], Sivaprakasam Radhakrishnan [d], Byoung-Suhk Kim [a,b,e*]

[a] *Department of Carbon Composites Convergence Materials Engineering, Jeonbuk National University, 567 Baekje-daero, Deokjin-gu, Jeonju-si, Jeollabuk-do 54896, Republic of Korea*

[b] *Department of JBNU-KIST Industry-Academia Convergence Research, Jeonbuk National University, 567 Baekje-daero, Deokjin-gu, Jeonju-si, Jeollabuk-do 54896, Republic of Korea.*

[c] *Research & Development Division, Korea Carbon Industry Promotion Agency, Jeonju 54853, Republic of Korea*

[d] *Department of Chemistry, School of Science and Humanities, SR University, Warangal 506371, Telangana, India.*

[e] *Department of Organic Materials and Textile Engineering, Jeonbuk National University, 567 Baekje-daero, Deokjin-gu, Jeonju-si, Jeollabuk-do 54896, Republic of Korea*

† Electronic supplementary information (ESI) available. See DOI: https://doi.org/10.1039/d4ta07531e

Corresponding Author. E-mail: kbsuhk@jbnu.ac.kr (Byoung-Suhk Kim)

Manufacturing process for S-ACs

1. Sample preparation

The coconut shell, purchased from a local market in Korea, was first crushed after being dried in a convection oven at 80°C. It was then washed several times with DI water to remove unbound dust, soil, and other water-soluble impurities. The washed coconut shell was then placed in a vacuum oven for 24 hrs before carbonization.

2. Carbonization

For the carbonization process, the coconut shell was heated to 700°C under a nitrogen (N_2) flow at a heating rate of 10°C/min using a lab-scale tube furnace, and held at this temperature for 1 hr before cooling down naturally.

3. Steam activation

3.0 g of the carbonized coconut shell was placed in an alumina boat and heated to 900°C under N_2 flow at a heating rate of 10 °C/min. The gas flow was then switched to steam at a flowing rate of 0.5 mL/min, and the temperature was maintained for 60 min. The sample was then cooled down to below 30 °C under N_2 flow. The obtained activated carbons (ACs) were used without any further purification.

ICP-OES analysis

An Inductively Coupled Plasma Optical Emission Spectrometer (iCAP 7400 Duo, Thermo Fisher Scientific) was utilized to analyze the concentration and elemental compositions of metallic and non-metallic impurities in ACs. To ensure accurate analysis, both Axial and

Radial View Modes were employed. The results were compared with those of Certified Reference Materials (CRMs). For the analysis, samples were pre-treated as follows,

1. Approximately 0.4 g of each sample was placed into a Teflon vessel.
2. 6 mL of concentrated nitric acid solution (~70%) and 0.5 mL of hydrofluoric acid solution (48%) were added to the vessel. The solutions were then treated using a microwave and heated to 250°C for 30 min, followed by cooling down.
3. The pre-treated solution was transferred to a 50 mL conical tube, and the final volume was adjusted to 50 mL with 2% nitric acid solution.

Here, it should be noted that the nebulizer and spray chamber of the ICP-OES were replaced with PTFE materials instead of quartz to prevent potential contamination during the analysis. Each element was measured three times, and the average value was reported.

Nitrogen adsorption-desorption measurements

To analyze the changes in specific surface areas and pore structure of ACs before and after purification, N_2 adsorption isotherm analysis was conducted using a BELSORP-mini-instrument (MicrotracBEL, Japan). For the analysis, 50 mg of activated carbon samples were pre-treated at 300°C for more than 12 hrs under vacuum to remove adsorbed moisture and air. The specific surface area (S_{BET}) and total pore volume (V_{total}) were calculated using the Brunauer-Emmett-Teller (BET) method. V_{total} was determined from measurements of the amount adsorbed at a relative pressure of p/p0 = 0.99. The average micropore diameters and micropore volume (V_{micro}) were calculated using the t-plot method. V_{micro} was obtained by fitting the linear range in the V_{ads}-t curve and calculating the positive intercept. The mesopore volume (V_{meso}) was determined by V_{total} -V_{micro} and the mesopore volume ratio (R_{meso}) was calculated as V_{meso}/V_{total}.

Preparation method for activated carbons with added impurities

1g of YP-50F was immersed in 50 mL of solutions prepared with NaCl, KCl, and $FeCl_2$ at a concentration of 0.01 wt%. After 1 hr of sonication treatment, the samples were aged at room temperature for 1 day and then dried in a convection oven at 80 ^{o}C for more than three days.

Table S1. Impurity elemental compositions in various ACs determined by ICP-OES.

ACs	Solution	Methodology	Elemental content analyzed by ICP-OES (ppm)																	
			Na	Mg	Al	P	K	Ca	Ti	Cr	Mn	Fe	Co	Ni	Cu	Sr	Sn	Ba	Si	Total
YP-50F	None		143	91	78	181	N.D	133	80	58	59	70	48	49	78	82	N.D	77	476	1703
S-ACs	None		1115	329	4128	480	9488	494	611	33	32	2114	N.D	18	31	29	8	46	7405	26361
	DI-water	1 time	248	212	4012	344	2015	454	589	23	31	2012	N.D	12	21	23	4	21	6808	16829
		5 times	73	211	3871	312	898	463	604	24	42	1988	N.D	4	17	12	3	41	6754	15317
		10 times	11	198	3912	310	3	433	585	21	28	1953	N.D	6	18	21	N.D	34	6312	13845
	HCl	0.01 mol	145	N.D	878	278	1213	78	142	N.D	N.D	332	N.D	N.D	N.D	N.D	N.D	24	1545	4635
		0.03 mol	235	N.D	1045	268	1101	76	121	N.D	12	478	N.D	N.D	N.D	N.D	N.D	32	1787	5155
		0.05 mol	212	N.D	1021	324	1227	108	131	N.D	7	499	N.D	N.D	7	N.D	2	12	2145	5695
		0.07 mol	224	N.D	1785	279	1354	145	137	21	N.D	875	N.D	1	N.D	N.D	N.D	33	2738	7592
		0.1 mol	212	N.D	1978	389	1412	212	188	17	N.D	1214	N.D	N.D	14	N.D	N.D	18	3065	8719
	NaOH	0.01 mol	412	265	2412	54	1743	304	598	N.D	34	575	N.D	N.D	N.D	N.D	N.D	N.D	971	7368
		0.03 mol	500	243	2986	21	1691	302	457	N.D	31	899	N.D	N.D	8	N.D	N.D	N.D	932	8070
		0.05 mol	798	311	3001	78	1729	287	578	N.D	45	876	N.D	N.D	N.D	N.D	N.D	N.D	1211	8914
		0.07 mol	1234	214	3012	45	1842	278	512	N.D	14	917	N.D	3	N.D	N.D	N.D	N.D	1787	9858
		0.1 mol	1543	308	2945	61	1994	239	567	N.D	12	925	N.D	N.D	N.D	N.D	N.D	N.D	2511	11105
	NaOH+HCl	0.01 mol	111	N.D	433	79	128	25	144	N.D	N.D	229	N.D	N.D	14	N.D	101	N.D	823	2087
		0.1 mol	310	144	1873	50	776	167	145	88	36	743	N.D	32	79	43	37	44	1586	6153

N.D : Not Detected.

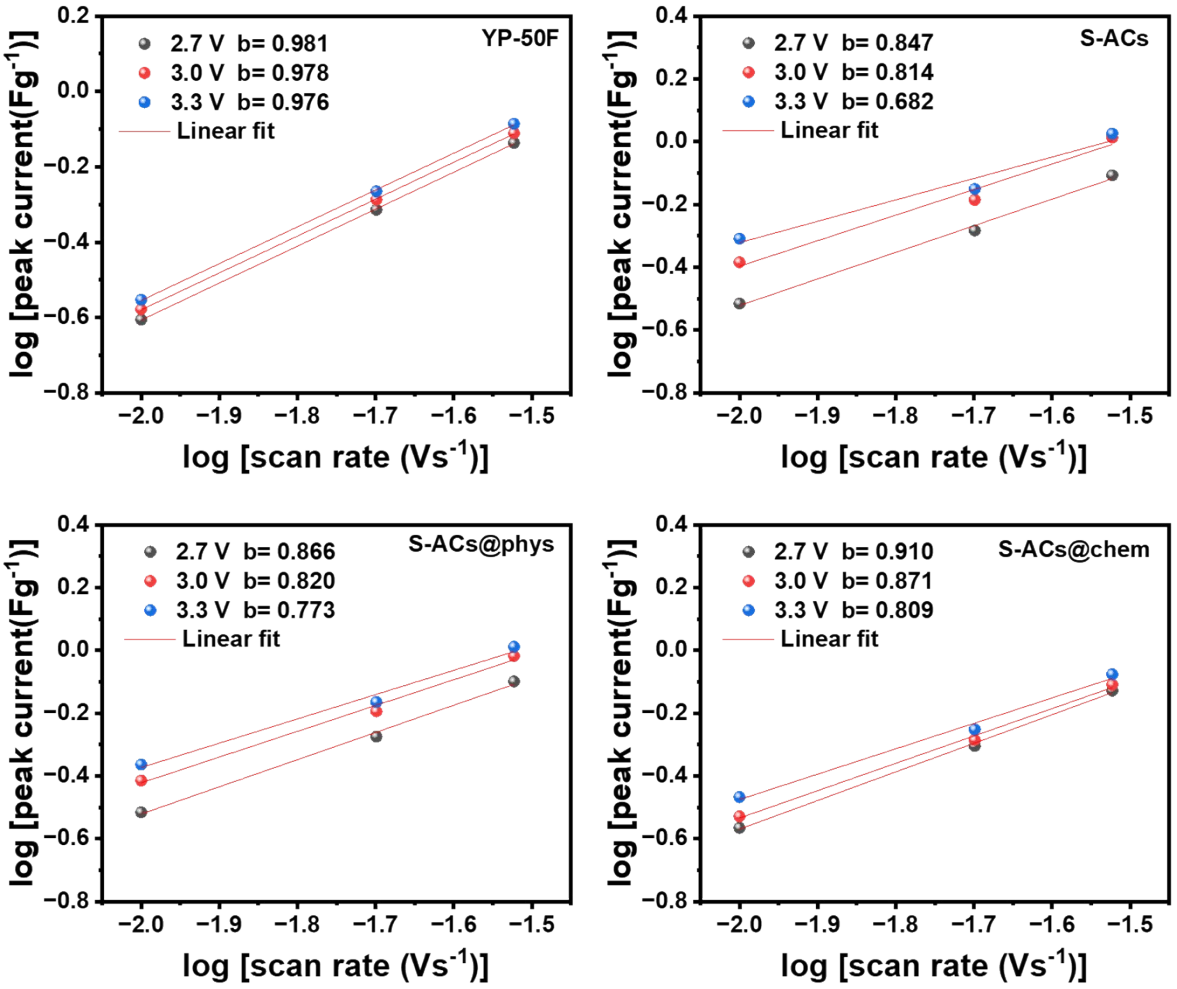

Fig. S1. logarithmic relationship between anodic scan rates and peak current ACs at different potentials.

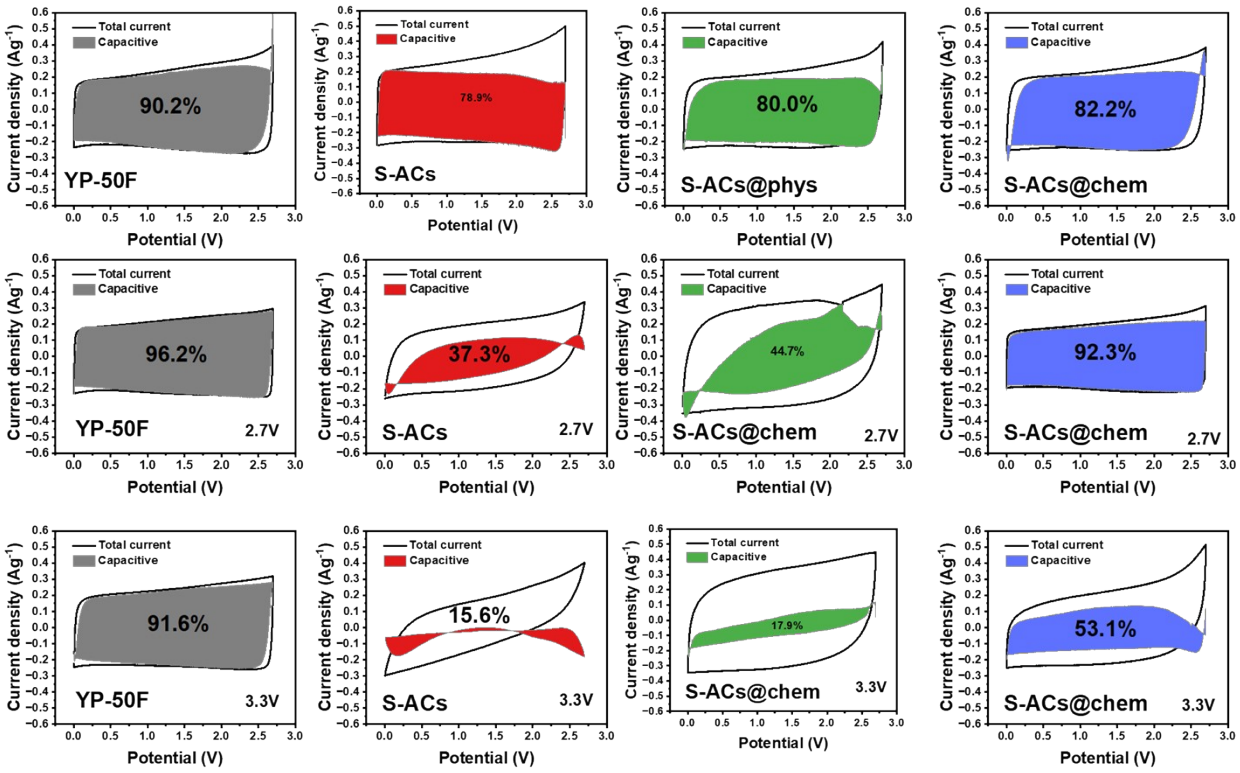

Fig. S2. The deconvolution of CV curves using Dunn`s method: before and after floating tests at 2.7V and 3.3V.

Table S2. Textural properties of various ACs.

ACs	YP-50F		S-ACs		S-ACs@phys		S-ACs@chem	
Electrode	+	-	+	-	+	-	+	-
S_{BETn} [a] (m^2/g)	1254.7	1374.7	229.4	348.6	531.2	590.9	698.5	801.4
V_{Total} [b] (cm^3/g)	0.6412	0.7575	0.1104	0.191	0.2461	0.3169	0.2885	0.3298
V_{micro} [c] ($cm^{3/g}$)	0.4789	0.5410	0.092	0.146	0.2041	0.2198	0.2734	0.3108
V_{meso} [d] (cm^3/g)	0.1623	0.2165	0.0184	0.0450	0.0420	0.0971	0.0151	0.0190
R_{meso} [e] (%)	23.4	28.6	16.7	13.6	17.1	30.6	5.2	5.8
Micropore diameter [f]	0.7134	0.7312	0.7384	0.6564	0.7023	0.6448	0.678	0.6304

[a] BET surface area.
[b] Total pore volume: the amount adsorbed $P/P_o = 0.99$.
[c] Micropore volume: t-plot.
[d] Mesopore volume: $V_{total}-V_{micro}$.
[e] Mesopore volume percentage: $V_{meso}/V_{total} \times 100$.
[f] Micropore diameter: t-plot

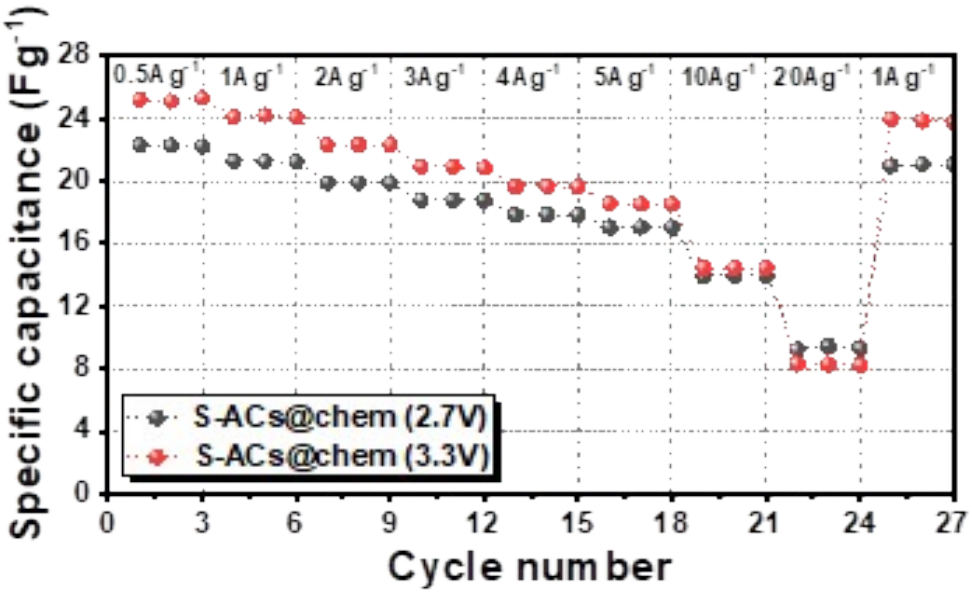

Fig. S3. Gravimetric capacitance of S-ACs@chem at different cell voltages (2.7 V and 3.3 V).

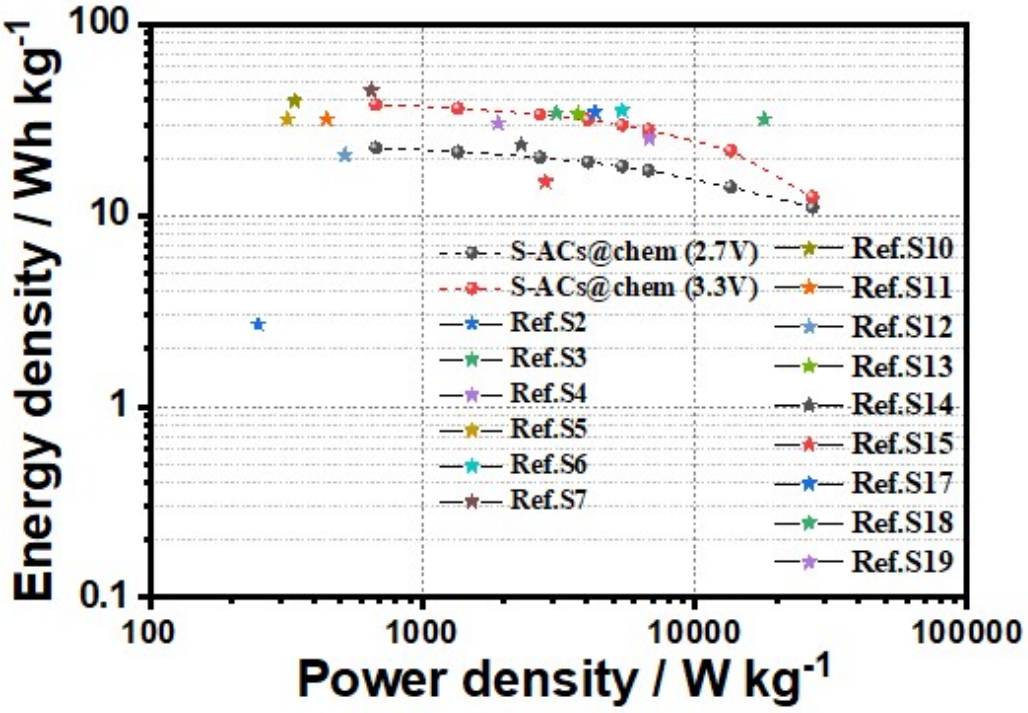

Fig. S4. Ragone plot of S-ACs@chem at different cell voltages (2.7 V and 3.3 V), compared with previous studies.

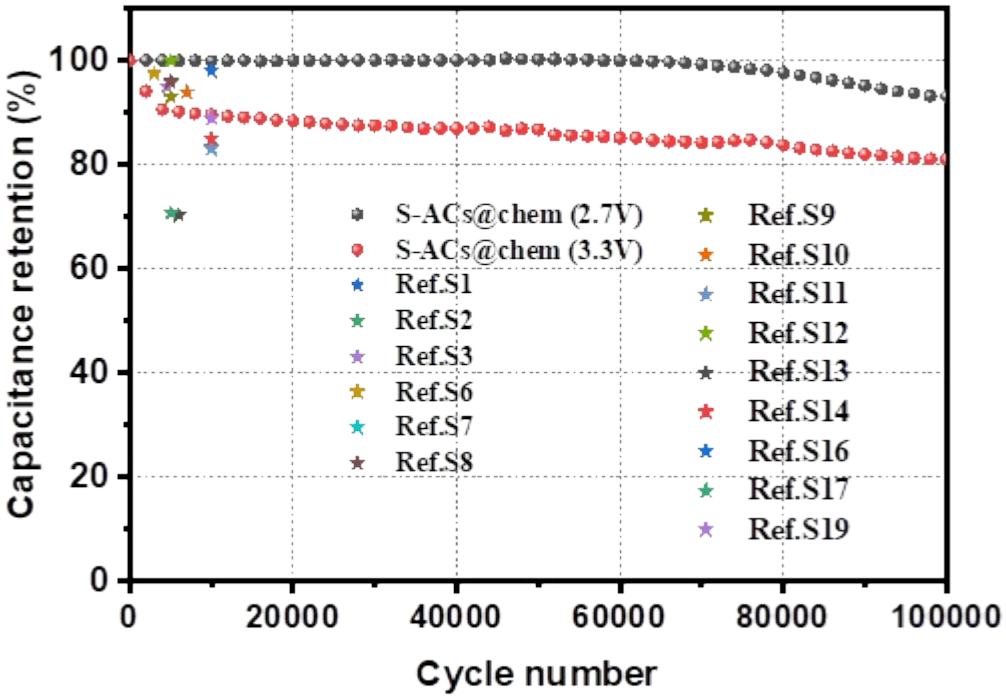

Fig. S5. Cycle stability of S-ACs@chem at different cell voltages (2.7 V and 3.3 V), compared with previous studies.

Table S3. Comparison of electrochemical performance of S-ACs@chem with previous studies.

Precursor	Activator	S_{BET} (m^2g)	Electrolyte	Cell voltage(V)	C_{sp} (Fg^{-1}) @ Current density (Ag^{-1})	ED (Wh/kg)	PD (W/kg)	Cycle number @ Cycling rate (Ag^{-1})	Retention (%)	Ref.
tree bark	KOH	1018	1 M Na_2SO_4	0.6	114 @ 0.3	-	-	5000 @ 5	100	S1
Pistachio shell	$Na_2S_2O_3$	775	1M KOH	1	88 @ 0.5	2.7	250	5000 @ 10	95.8	S2
Silkworm cocoon	KOH	3386	1 M $TEABF_4$ in ACN	2.5	156.1@ 5	34.4	3100	4500@20	95	S3
Argan shells	KOH	2251	1 M $TEABF_4$ in ACN	2.5	ca.36	30.5	1900	-	-	S3
Durian husk	KOH	2488	1 M $TEABF_4$ in ACN	2.5	145	32	320	-	-	S5
Samanea saman leaves	KOH	2930	1 M $TEABF_4$ in ACN	2.5	179.2	35.3	5410	3000 @ 5	97.5	S6
Potatoes	KOH	1381	$BMIMBF_4$ in ACN	2.6	182 @ 0.5	45.1	650	10000 @ 5	83.3	S7
Pollens from lotus	KOH	3037	1 M $TEABF_4$ in ACN	2.7	185 @ 1	46	-	5000 @ 1	96	S8
Sawdust	KOH	2924	1 M $TEABF_4$ in ACN	2.5	150 @ 0.25	44	-	5000 @ 0.5	93	S9
Pollen pine	KOH	2318	1 M $TEABF_4$ in ACN	2.5	147 @ 0.5	39.7	340	7000 @ 1	94	S10
Pear	KOH	2332	1 M $TEABF_4$ in ACN	2.5	126 @ 2	32	445	10000 @ 2	83	S11
Potato	Self activation	2201	1 M $TEABF_4$ in ACN	2.1	34.0 @ 0.5	20.8	520	5000 @ 5	~100	S12
Spent coffee grounds	CO_2	2497	1.5 M $LiClO_4$/PC	2.5	222.4 @ 0.5	33.8	3730	6000 @ 1	70.3	S13
Bamboo bagasse	$ZnCl_2$ +CO_2	-	1 M $TEABF_4$ in ACN	2.7	153 @ 1	23.5	2300	10000	85	S14
Corncob residue	Steam	1210	1M $TEABF_4$ in ACN	-	120 @ 1	15	2827	-	-	S15
Soybean waste	Steam	1321	1M Na_2SO_4	1	151.5 @ 1	-	-	10000	98	S16
Plane tree bark	ZnO	1511	1 M $TEABF_4$ in ACN	3.0	115 @ 20	34.6	4300	5000 @ 2	70.8	S17
Eucalyptus sawdust	KCl/$Na_2S_2O_3$	2590	1 M $TEABF_4$ in ACN	2.7	140 @ 5	32	18000	-	-	S18
Lignin	K_2CO_3	1529	1 M $TEABF_4$ in ACN	2.5	140 @ 0.05	25.3	6800	10000 @ 5	89	S19
Coconut shell (S-ACs @ chem)	Steam	1341	1 M $DMPBF_4$ in ACN	2.7	22.2 @ 0.5	22.6 9.5	675 27000	100000 @ 5	93	This work
				3.3	25.2 @ 0.5	38.1	675	53896 @ 5	80	

8.2 27000

Table S4. Impurity elemental compositions in YP-50F and impurity-added YP-50F determined by ICP-OES

Commercial ACs	Elemental content analyzed by ICP-OES (ppm)																	
	Na	Mg	Al	P	K	Ca	Ti	Cr	Mn	Fe	Co	Ni	Cu	Sr	Sn	Ba	Si	Total
YP-50F	143	91	78	181	0	133	80	58	59	70	48	49	78	82	0	77	476	1703
YP-50F + NaCl	11778	14	99	20	348	127	0	0	1	4	0	1	25	0	0	4	848	13269
YP-50F + KCl	167	24	57	23	12810	128	0	1	0	689	0	12	37	0	0	2	732	14682
YP-50F + $FeCl_2$	122	87	21	78	121	145	0	51	4	9312	11	0	54	54	0	11	675	10746

References

1. D. Momodu, M. Madito, F. Barzegar, A. Bello, A. Khaleed, O. Olaniyan, J. Dangbegnon, N. Manyala, *J. Solid State Electrochem.*, 2017, **21**, 859.
2. O. C. Altinci, M. Demir, *Energy & Fuels*, 2020, **34**, 7658-7665.
3. J. Sun, J. Niu, M. Liu, J. Ji, M. Dou, F. Wang, *Appl. Surf. Sci.*, 2018, **427**, 807-813.
4. O. Boujibar, A. Ghosh, O. Achak, T. Chafik, F. Ghamouss, *J. Energy Storage*, 2019, **26**, 100958.
5. P. Ukkakimapan, V. Sattayarut, T. Wanchaem, V. Yordsri, M. Phonyiem, S. Ichikawa, M. Obata, M. Fujishige, K. Takeuchi, W. Wongwiriyapan, M. Endo, *Diam. Relat. Mater.*, 2020, **107**, 107906.
6. V. Sattayarut, T. Wanchaem, P. Ukkakimapan, V. Yordsri, P. Dulyaseree, M. Phonyiem, M. Obata, M. Fujishige, K. Takeuchi, W. Wongwiriyapan, M. Endo, *RSC Adv.*, 2019, **9**, 21724-21732.
7. C. Lu, X.-Z. Qian, H.-Y. Zhu, Y.-X. Hu, Y.-S. Zhang, B.-M. Zhang, L.-B. Kong, M.-C. Liu, *Mater. Res. Express*, 2019, **6**, 115615.
8. L. Zhang, F. Zhang, X. Yang, K. Leng, Y. Huang, Y. Chen, *Small*, 2013, **9**, 1342-1347.
9. O. E. Eleri, K. U. Azuatalam, M. W. Minde, A. M. Trindade, N. Muthuswamy, F. Lou, Z. Yu, *Electrochim. Acta*, 2020, **362**, 137152.
10. Y. Myung, S. Jung, T. T. Tung, K. M. Tripathi, T. Kim, *ACS Sustain. Chem. Eng.*, 2019, **7**, 3772-3782.
11. W. Fan, H. Zhang, H. Wang, X. Zhao, S. Sun, J. Shi, M. Huang, W. Liu, Y. Zheng, P. Li, *RSC Adv.*, 2019, **9**, 32382-32394.
12. A. Wang, K. Sun, R. Xu, Y. Sun, J. Jiang, *J. Clean. Prod.*, 2021, **283**, 125385.
13. T.-H. Hsieh, H.-L. Wang, G.-T. Yu, G.-M. Huang, J.-H. Lin, *J. Environ. Chem. Eng.*, 2021, **9**, 106418.
14. S. Sundari Gunasekaran, R. Subashchandra Bose, K. Raman, *Orient. J. Chem.*, 2019, **35**, 302-307.
15. W.-H. Qu, Y.-Y. Xu, A.-H. Lu, X.-Q. Zhang, W.-C. Li, *Bioresource Technology*, 2015, **189**, 285-291.
16. Wei Sun, Yan Xiao, Qingyuan Ren, Fuqian Yang, *Journal of Energy Storage*, 2020, ***27***, 101070,
17. F. Yu, Z. Ye, W. Chen, Q. Wang, H. Wang, H. Zhang, C. Peng, [Journal and year not provided] Plane tree bark-derived mesopore-dominant hierarchical carbon for high-voltage supercapacitors
18. M. Sevilla, N. Diez, G. A. Ferrero, A. B. Fuertes, *Energy Storage Mater.*, 2019, **18**, 356-365.
19. Y. Zhang, B. Yu, J. Zhang, X. Ding, J. Zeng, M. Chen, C. Wang, *ChemElectroChem*, 2018, **5**, 2142-2149.